A study of hydrodynamically lubricated contact between axial rings of a high-speed gearbox

Cite as: AIP Conference Proceedings **2323**, 020001 (2021); https://doi.org/10.1063/5.0042747
Published Online: 08 March 2021

Josef Voldřich and Štefan Morávka

A Study of Hydrodynamically Lubricated Contact between Axial Rings of a High-Speed Gearbox

Josef Voldřich[1, 2, a)] and Štefan Morávka[1, b)]

[1]*University of West Bohemia, New Technologies – Research Centre, Univerzitní 8, 30100 Plzeň, Czech Republic*
[2]*University of West Bohemia, Faculty of Mechanical Engineering, Department of Power System Engineering, Univerzitní 8, 30100 Plzeň, Czech Republic*

[a)]Corresponding author: voldrich@ntc.zcu.cz
[b)]moravka@ntc.zcu.cz

Abstract. The paper investigates the pressure field and losses in hydrodynamically lubricated contact between axial rings of the pinion and the wheel of a high-speed gearbox under steady-state load. For that reason, a computer program was developed to numerically solve the general Reynolds and energy equations simultaneously, while considering the viscosity-temperature relationship. The Barus empirical equation was used to express a viscosity-pressure relationship as well. For the selected design parameters, dissipative heat in the lubricated contact is shown as a function of transmitted axial force. It is presented that the contact axial force and losses are affected by procedure of the filling of the gap between the rings.

INTRODUCTION

High-speed gearboxes are used in the power engineering sector, particularly in gas and steam turbine drives, turbo compressors and auxiliary starting drives. A present-day requirement for such gearboxes is to achieve their mechanical efficiency of no less than 99%. Since low-speed shaft bearings generate lower losses than their high-speed counterparts, the axial bearing of a pinion shaft is replaced by axial rings for the transmission of axial forces from the high-speed shaft to the low-speed shaft. Nevertheless, friction losses need to be taken into account even between the axial rings. In addition to rolling, the slipping of rings occurs due to the shift of their contact center out of the pitch contact circles. Figure 1 shows an example of a pinion design.

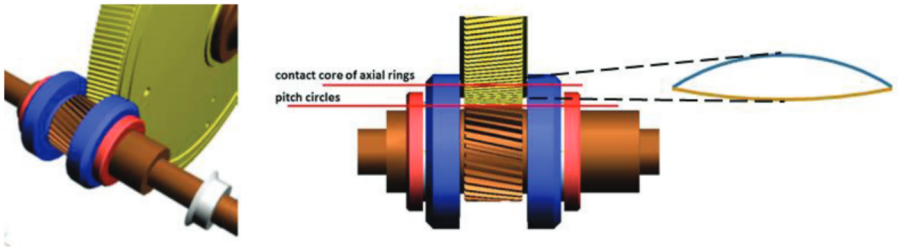

FIGURE 1. A 3D pattern with a pinion and a wheel and with the enlarged overlap of their rings.

To keep the friction losses as low as possible, the parameters of the rings must be appropriately designed for the required power transmission in the given operating mode. To do this, it is desirable to know how changes in geometric parameters of the rings, in the operating parameters and oil properties affect the size of those losses.

The subject of hydrodynamic lubrication as applied to journal bearings is well developed [1, 2, 3, 4]. However, it seems that no pertinent research paper dealing with the lubricated contact of axial rings has been published so far. The lack of specific knowledge represents an obstacle towards future development of the rings and towards an increase of

19th Conference on Power System Engineering
AIP Conf. Proc. 2323, 020001-1–020001-12; https://doi.org/10.1063/5.0042747
Published by AIP Publishing. 978-0-7354-4067-8/$30.00

the power transmitted through the gearbox while observing a high efficiency rating. The paper particularly focuses on numerical analysis of the pressure field and losses in the contact between the rings. The general Reynolds and energy equations are used to propose an appropriate mathematical model. A viscosity-temperature relation and the Barus empirical formula [5] are considered simultaneously. The model is completed by the Kapitza condition for the subject of cavitation. Perfect geometry of the rings is assumed. The assumption of the contact being hydrodynamically lubricated is suitable as the ratio between the minimal oil film thickness, $h_{\min}$, and roughness of surfaces, σ, conforms to the precondition $h_{\min}/\sigma >> 3$ (see e.g. [6]).

It is the purpose of this paper to present the axial contact force and the energy losses as functions of design parameters, in particular in terms of the nominal film thickness. Consequently, the dissipative heat in the lubricated contact is shown as a function of transmitted axial force for the selected design parameters. At the same time, two extreme cases are discussed. In the first case, the isothermal condition is considered for the oil film. In the second one, an adiabatic boundary condition is assumed on the surfaces of the rings. An in-house program was developed to perform the numerical calculations mentioned above.

NOMENCLATURE

F	contact axial force between the rings
h	film thickness, $h = h_w + h_p$
h_p	distance between a pinion ring point and the reference plane
h_w	distance between a wheel ring point and the reference plane
p	pressure
x, y, z	coordinates in the global coordinate system
x	direction in the plane of shaft axes
z	pinion shaft axial direction in global coordinate system
ξ, η, ψ	Cartesian coordinates relative to the contact reference plane
ξ	direction perpendicular to the contact reference plane
χ	direction of the intersection of shaft axes with the contact reference plane
T	oil film temperature
T_0	inlet oil temperature
u	fluid velocity in the χ direction
v	fluid velocity in the ψ direction
w	fluid velocity in the ξ direction
η	oil dynamic viscosity
μ_0	oil kinematic viscosity at atmospheric pressure
μ	oil kinematic viscosity
α	parameter in the Barus equation
ρ	oil density
$\pi/2 - \varphi$	conicity of the pinion ring
$\pi/2 - \phi$	conicity of the wheel ring
ω	angular frequency of the pinion shaft
Ω	angular frequency of the wheel shaft

Subscripts

p	surface of the pinion
w	surface of the wheel

THEORY

The theoretical foundation of lubricated journal bearings has been presented in detail elsewhere [1, 2]. We apply this methodology to the case of conical axial rings. In addition, it is necessary to pay attention to the geometry and kinematics of the oil film between the rings. Some detailed derivation of the necessary relationships and equations is carried out in the report [7]. Only the general scheme is presented in this paper.

Gap between Axial Rings and Film Thickness

Cross-sections of lubricated contact between conical rings showing the nomenclature of the problem are presented in Figures 2 and 3.

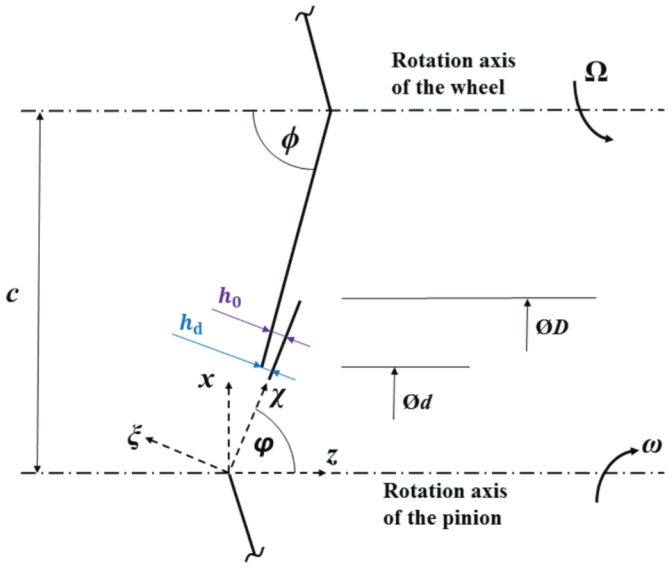

FIGURE 2. Scheme of the cross-section of beveled rings with the nomenclature of geometric parameters and coordinate systems employed

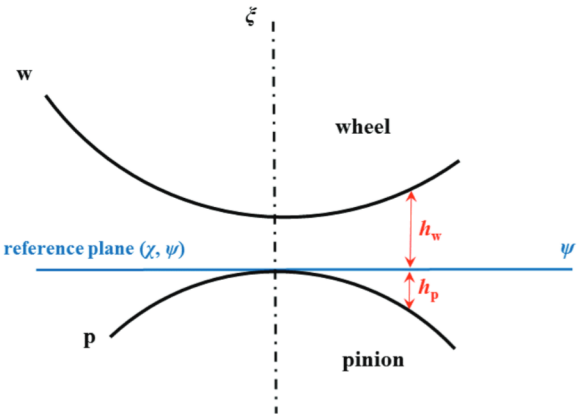

FIGURE 3. Scheme of the cross-section perpendicular to the reference plane

The thickness of the oil film between the rings is considered in the direction perpendicular to the reference plane (χ,ψ). The nominal film thickness, h_0, belongs to the point in the center of the contact, i.e. to the point of the reference plane with $\xi = 0$, $\chi = (d+D)/2$ and $\psi = 0$ (see Fig. 2). For the needs of a mathematical model, we further consider the distances of points of the pinion and wheel surfaces from the reference plane, $h_p = h_p(\chi,\psi)$, $h_w = h_w(\chi,\psi)$, $h = h_p + h_w$, (see Fig. 3). As in the report [7], we can derive the formulae

$$h_p = -\frac{1}{2A}\left(-B+\sqrt{B^2-4AC}\right), \qquad h_w = \frac{1}{2S}\left(-T+\sqrt{T^2-4SU}\right),$$

where

$$A = \cos^2\varphi - \sin^2\varphi \ tg^2\varphi\,, \qquad S = \cos^2\varphi - \sin^2\varphi \ tg^2\phi\,,$$

$$B = 2\chi\cos\varphi\sin\varphi\,(1+tg^2\phi)\,, \qquad T = 2\chi\cos\varphi\sin\varphi\,(1+tg^2\phi) - 2c\cos\varphi - 2f\sin\varphi\,tg^2\phi\,,$$

$$C = \psi^2\,, \qquad U = (-\chi\sin\varphi + c)^2 + \psi^2 - (-\chi\cos\varphi + f)^2 tg^2\phi\,,$$

$$f = b - h_d\sin\varphi + d/2tg\varphi$$

General Reynolds Equation

Referring to Figures 2 and 3, we consider the following assumptions to obtain the general Reynolds equation from the Navier-Stokes equations:

1) The thickness of the fluid film h is very small compared to the width and length of χ, ψ.
2) Pressure is constant across the fluid film. Therefore, $\partial p / \partial \xi = 0$.
3) The lubricant is a Newtonian fluid, and its flow is laminar and steady-state.
4) Inertia of the fluid is small compared to the viscous shear and pressure effects.
5) No external forces act on the film.
6) No slip occurs at the surfaces of the rings.
7) Compared with the two velocity derivations $\partial u / \partial \xi = 0$ and $\partial v / \partial \xi = 0$, all other velocity derivations are negligible.

These assumptions used in the Navier-Stokes equations offer

$$\frac{\partial p}{\partial \chi} = \frac{\partial}{\partial \xi}\left(\eta\frac{\partial u}{\partial \xi}\right), \qquad \frac{\partial p}{\partial \psi} = \frac{\partial}{\partial \xi}\left(\eta\frac{\partial v}{\partial \xi}\right)$$

By integrating these derivatives twice with the boundary conditions for velocities on the surfaces of the rings, we receive

$$u(\xi,\chi,\psi) = \frac{1}{2\eta}\frac{\partial p}{\partial \chi}\left\{\xi^2 - \xi\,(h_w - h_p) - h_w h_p\right\} + u_w\frac{\xi + h_p}{h} + u_p\frac{h_p - \xi}{h}, \quad -h_p \le \xi \le h_w,$$

$$v(\xi,\chi,\psi) = \frac{1}{2\eta}\frac{\partial p}{\partial \psi}\left\{\xi^2 - \xi\,(h_w - h_p) - h_w h_p\right\} + v_w\frac{\xi + h_p}{h} + v_p\frac{h_w - \xi}{h}, \quad -h_p \le \xi \le h_w$$

The general Reynolds equation can now be derived by integrating the continuity equation across the fluid film [1, 2]. In the case of an uncompressible fluid, we obtain

$$\frac{\partial}{\partial \chi}\left(\frac{\rho h^3}{12\eta}\frac{\partial p}{\partial \chi}\right) + \frac{\partial}{\partial \psi}\left(\frac{\rho h^3}{12\eta}\frac{\partial p}{\partial \psi}\right) = \frac{\partial}{\partial \chi}\left(\frac{\rho h(u_p + u_w)}{2}\right) + \frac{\partial}{\partial \psi}\left(\frac{\rho h\,(v_p + v_w)}{2}\right) +$$

$$+ \rho(w_w - w_p) - \rho u_w\frac{\partial h_w}{\partial \chi} - \rho u_p\frac{\partial h_p}{\partial \chi} - \rho v_w\frac{\partial h_w}{\partial \psi} - \rho v_p\frac{\partial h_p}{\partial \psi}$$

(The sum of the third to last term of the right-hand site turns out to be very small.) Oil viscosity, η, is a function of both temperature and pressure. For a specific oil, the dependence of viscosity on temperature is based on measurement results. The Barus empirical formula $\mu = \mu_0 \exp(\alpha p)$ then describes the dependence of viscosity on pressure. In such case, the Reynolds equation is nonlinear, and we need to apply an iterative method to solve the Reynolds equation. However, from a purely mathematical point of view, in the case of steep and unlimited exponential growth, the

existence of a solution of the equation is not guaranteed. This can lead to problems with the convergence of numerical iterations for marginal cases, e.g. those with a very low thickness of the fluid film, h .

Besides, the mathematical model described requires being completed with a condition for cavitation. Here, the simple approach taken by Kapitza that ignores the negative pressure, i.e. $p \geq 0$, is considered [1]. As the pressure of the oil film can reach up to dozens of MPa, zero pressure value is taken as a boundary condition instead of atmospheric pressure.

Dissipative Heat

We can derive an equation for the density of the rate of fluid kinetic energy. Multiplying the Navier-Stokes equation by the velocity vector and rearranging terms offers the following [7, 8]:

$$\rho\frac{\partial(a^2/2)}{\partial t} = -\rho\frac{\partial}{\partial x_\mathrm{i}}\left(\frac{a_\mathrm{i}a^2}{2}\right) - \frac{\partial(a_\mathrm{i}p)}{\partial x_\mathrm{i}} + \frac{\partial(a_\mathrm{i}\tau_{\mathrm{ij}})}{\partial x_\mathrm{j}} - \tau_{\mathrm{ij}}S_{\mathrm{ij}} \tag{1}$$

where summation over the repeated indexes i, j is assumed. Here $\vec{a} = (a_1, a_2, a_3) = (w, u, v)$ is the velocity vector, $a = |\vec{a}|$, $(x_1, x_2, x_3) = (\xi, \chi, \psi)$. S_{ij} is the strain rate tensor, $S_{\mathrm{ij}} = \frac{1}{2}\left(\frac{\partial a_i}{\partial x_j} + \frac{\partial a_j}{\partial x_i}\right)$, and $\tau_{\mathrm{ij}} = 2\eta S_{\mathrm{ij}}$ denote the tensor of shear stresses. The left-hand side of the equation (1) is zero for the steady state. The last term of the right side represents the density of dissipative energy which, in view of the above assumptions 1-7, can be reduced to

$$\tau_{\mathrm{ij}}S_{\mathrm{ij}} = 2\eta S_{\mathrm{ij}}S_{\mathrm{ij}} \approx \eta\left[\left(\frac{\partial u}{\partial \xi}\right)^2 + \left(\frac{\partial v}{\partial \xi}\right)^2\right]$$

with only little error. Integrating across fluid film we obtain the plane density of the rate of dissipative heat

$$\int_{-h_p}^{h_w} \tau_{\mathrm{ij}}S_{\mathrm{ij}}\,\mathrm{d}\xi \approx \frac{h^3}{12\eta}\left[\left(\frac{\partial p}{\partial \chi}\right)^2 + \left(\frac{\partial p}{\partial \psi}\right)^2\right] + \frac{\eta}{h}(u_w - u_p)^2 + \frac{\eta}{h}(v_w - v_p)^2 = e(\chi, \psi) \tag{2}$$

Volume-based integration over fluid film in the equation (1) can also be applied. By the divergent theorem, volume integrals of the first three members of its right side can be converted to surface integrals. The first member then represents the flux of kinetic energy across the boundary of a fluid film model. However, this flux is extremely low as values of integrals over the ring surfaces are zero. No fluid flow is crossing those surfaces. For the same reason and for the fact that pressure is zero in the open parts of the film boundary, the contribution of the second member is very low as well. After conversion to the surface integral, the third member of the right side (1) represents the rate at which the viscous forces do work (through the solid surfaces of rings). We can find the corresponding surface density of the rate [7]

$$a_\mathrm{i}\tau_{\mathrm{ij}}n_\mathrm{j} \approx \frac{h}{2}(u_w - u_p)\frac{\partial p}{\partial \chi} + \frac{h}{2}(v_w - v_p)\frac{\partial p}{\partial \psi} + \frac{\eta}{h}(u_w - u_p)^2 + \frac{\eta}{h}(v_w - v_p)^2 \tag{3}$$

Here n_j denotes the j-th component of the normal vector to surface. Under steady conditions, the rate of working of the forces is dominantly balanced by viscous dissipation within the fluid film. Despite this balance, the densities (2), (3) may be different locally due to their parts with pressure gradient.

Film Temperature Field

We consider constant temperature, T , across the fluid film thickness. Therefore, it is beneficial to integrate the heat transfer equation [2] across the film thickness as well. This gives

$$c\rho\left(h\frac{\partial T}{\partial t}+q_{\chi}\frac{\partial T}{\partial \chi}+q_{\psi}\frac{\partial T}{\partial \psi}\right)=e(\chi,\psi)-F(T,h,\lambda,T_S)$$

where q_{χ}, q_{ψ} are volume fluxes per unit of length in the χ and ψ directions, respectively. Plane density of the rate of dissipative heat, $e(\chi,\psi)$, is expressed by (2). External cooling of the fluid film is described by the term $F(T,h,\lambda,T_S)$ in which T_S denotes the temperature of the rings while λ is the thermal conductivity of the lubricant. However, we will only conservatively investigate the adiabatic solution and consider no heat flow across the boundary between the film and the rings. Therefore, the last term will be omitted.

RESULTS AND DISCUSSION

An in-house program was developed to perform the numerical calculations. Pressure distribution and the temperature field in the reference plane are obtained by appropriate iterative techniques. The finite element method is employed to solve the general Reynolds equation while the temperature field is solved by the finite volume method. Negative pressure values are set equal to zero when they appear in the iterations. The centers of these finite volumes are the FEM nodes.

The main effort is devoted to quantifying the axial contact force and friction losses. Two examples are given here for illustration, both with the following operational parameters: D = 180 mm, d = 125 mm, c = 450 mm, $\varphi = \Phi$ = 89°, ω = 10,791.2 rpm, Ω = 1,490 rpm, α = 0.02149 MPa^{-1}. Nominal thickness h_0 uses variable values. Kinematic viscosity as the function of temperature is assumed to be defined by the empirical formula for the oil of VG 46 under a negligible reference pressure: $\mu_0 = 0.232\text{x}10^{-5}*T^4 - 0.844\text{x}10^{-3}*T^3 + 0.1197*T^2 - 8.005*T + 222.38$ Pa.s. The examples differ in the method of filling the gap between the rings.

Example 1 – The Gap between the Rings Filled Completely

In this example, the gap between the rings is filled with oil completely. Figure 4 shows thickness distribution between the rings for the nominal value h_0 = 0.03 mm. The velocity fields of the pinion and wheel surface are given in Figure 5. We can see that the maximum slipping of rings occurs in the longitudinal direction ψ of their overlap area.

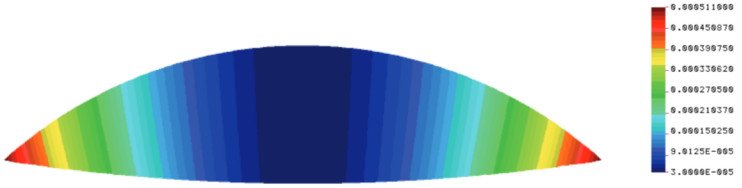

FIGURE 4. Oil film thickness for parameters h_0 = 0.03 mm, D = 180 mm, d = 125 mm, c = 450 mm, $\varphi = \Phi$ = 89°. Scale from 0.03 mm to 0.51 mm.

Following the monograph [1], we can estimate the modified Reynolds number by analogy as for a typical journal bearing:

$$\text{Re} = \frac{\rho u h_o^2}{\eta L} = \frac{(866\text{kg m}^{-3})(50\text{ms}^{-1})(0.03\times10^{-3}\text{ m})^2}{(0.04\text{ Pa.s})(0.035\text{ m})} = 2.8\times10^{-2}$$

Here u represents a characteristic velocity and L a characteristic length. The Reynolds number is considerably lower than one, i.e. the viscous forces encountered in the lubrication are much greater than the inertia forces. Therefore, the use of the Reynolds equation is appropriate.

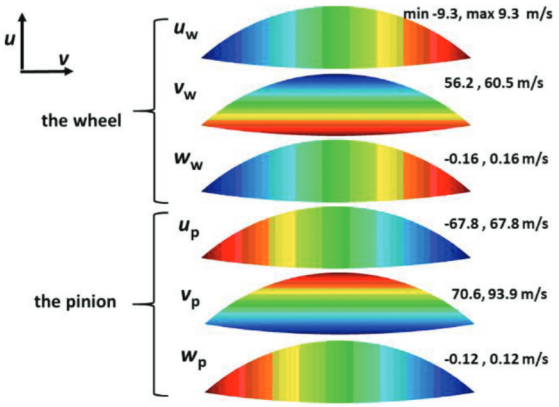

FIGURE 5. Fields of surface velocities of the pinion and wheel rings with parameters from Fig. 4 and with angular frequencies ω = 10,791.2 rpm, Ω = 1,490 rpm.

Figure 6a shows the values of axial contact force versus nominal film thickness both for the isothermal (black lines) and for the adiabatic assumptions (red lines). In the isothermal case, the temperature considered is 40° C. Solid lines are obtained for the Barus parameter α = 0.02149, dashed lines for its value of α = 0.0. Identical marking is used for Figure 6b on which dependencies of friction losses on the nominal film thickness are shown for the cases being considered.

Figures 7 to 11 are the results of calculations for the nominal film thickness of 0.03 mm. Figure 7 gives pressure distribution in the fluid film both for the isothermal and for the adiabatic assumptions. The total axial contact force is calculated by integrating this distribution over the area of the fluid film. In the case of the adiabatic assumption, the maximum pressure is approximately half that of the isothermal case. Special attention should be given to Figure 8 with the distribution of the rate of dissipative heat that is qualitatively different from the rate of working (see Figure 9). The rate of dissipative heat (friction losses) affects the temperature distribution, as shown by comparison of Figures 8 and 10.

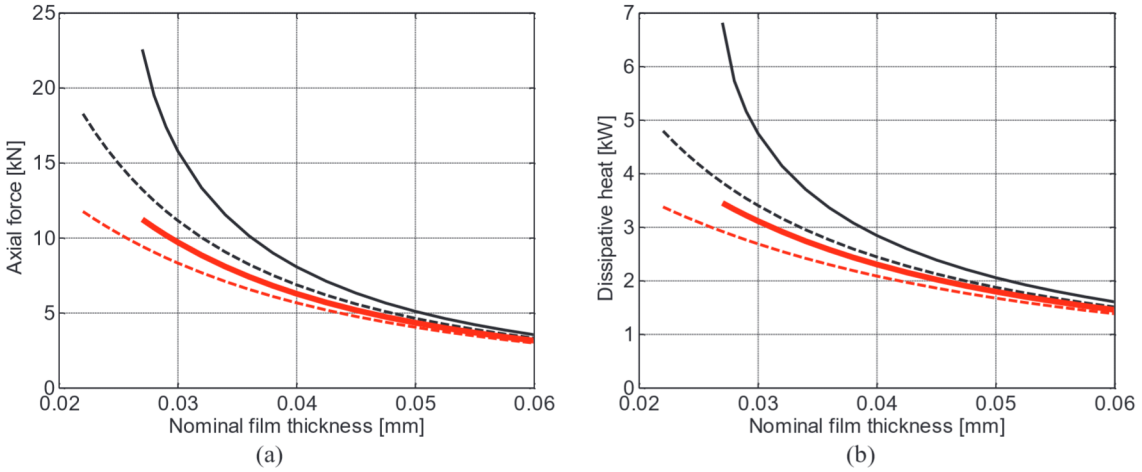

FIGURE 6. (a) Axial contact force as a function of the nominal film thickness h_0, (b) dissipative heat in the contact as a function of the nominal film thickness h_0. Full lines – the Barus coefficient α = 0.02149, dashed lines - α = 0. Black lines –film viscosity for T = 40°C, red lines –film viscosity as the function of temperature T for the adiabatic assumption.

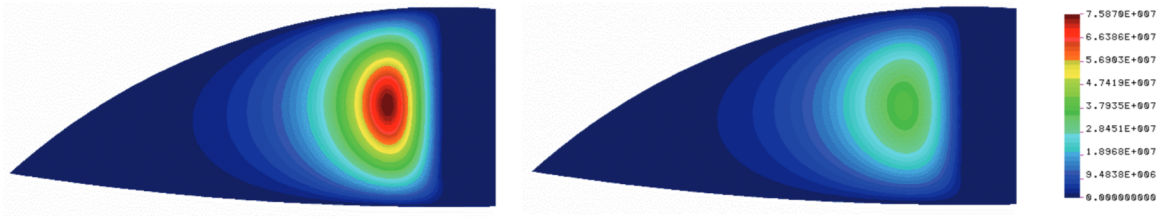

(a) (b)

FIGURE 7. Pressure field of the oil film for: (a) the isothermal assumption with T = 40°C, (b) the adiabatic assumption. Color scale from 0 to 75.9 MPa.

(a) (b)

FIGURE 8. Planar density of the rate of dissipative heat for: (a) the isothermal assumption with T = 40°C, (b) the adiabatic assumption. Color scale from 0 to 11.6 MW/m^2. The area without cavitation is 1.13x10^{-3} m^2.

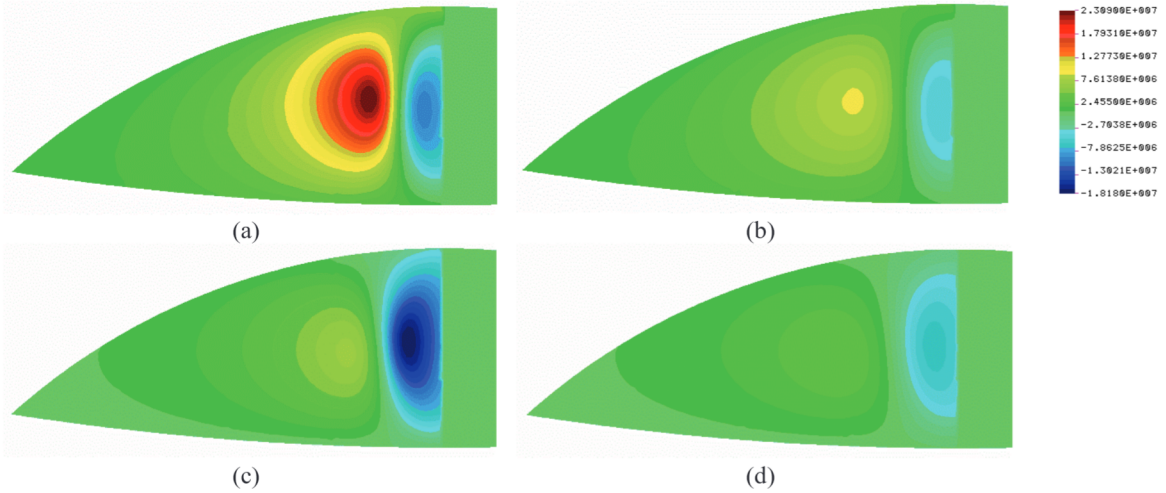

(a) (b)

(c) (d)

FIGURE 9. Planar density for the rate of working of a ring surface: (a), (c) the isothermal assumption with T = 40°C, (b), (d) the adiabatic assumption; (a), (b) the pinion, (c), (d) the wheel. Color scale from -18.2 to 23.1 MW/m^2.

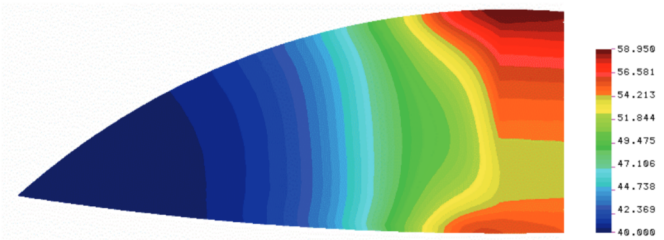

FIGURE 10. Temperature field in the adiabatic case. Color scale from 40.0 to 59.0°C.

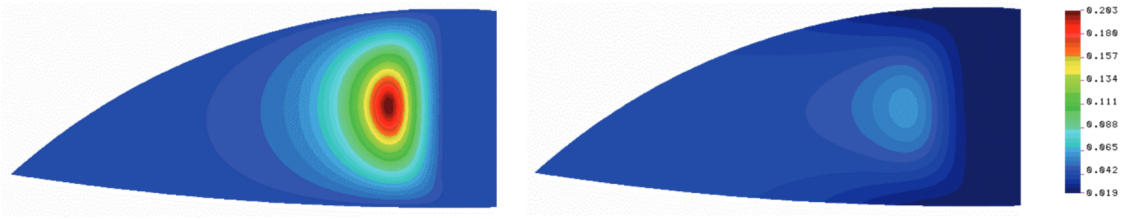

(a) (b)

FIGURE 11. Distribution of dynamic viscosity for: (a) the isothermal assumption with T = 40°C, (b) the adiabatic assumption. Color scale from 0.019 to 0.203 Pa.s.

Example 2 – The Gap between the Rings Filled In Part

In this example, the gap between the rings is filled with oil only in part (see Figure 13). All other operating parameters are identical to the first case. Although the results may seem qualitatively similar to those of the first example, as Figures from 12 to 17 show, axial contact forces are significantly lower for the same nominal thicknesses, by as much as 50%. However, the crucial result is that the transmission of the same axial contact force in the second example with the gap filled only in part shows friction losses which are significantly lower than in the first example. The quantitative comparison is done in Figure 18. (Figures from 13 to 17 are obtained for a nominal thickness of 0.03 mm.)

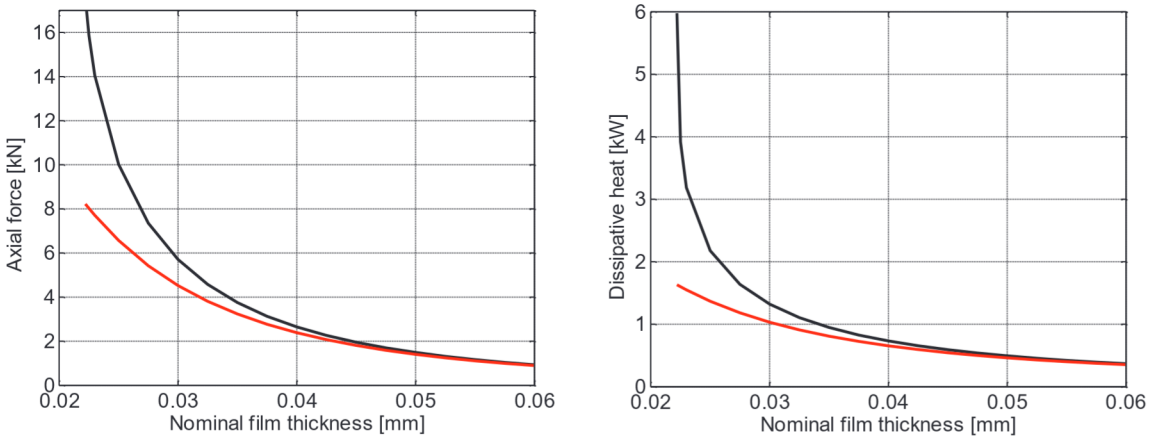

(a) (b)

FIGURE 12. (a) Axial contact force as a function of the nominal film thickness h_0, (b) dissipative heat in the contact as a function of the nominal film thickness h_0. Black lines –film viscosity for T = 40°C, red lines –film viscosity as a function of temperature T for the adiabatic assumption.

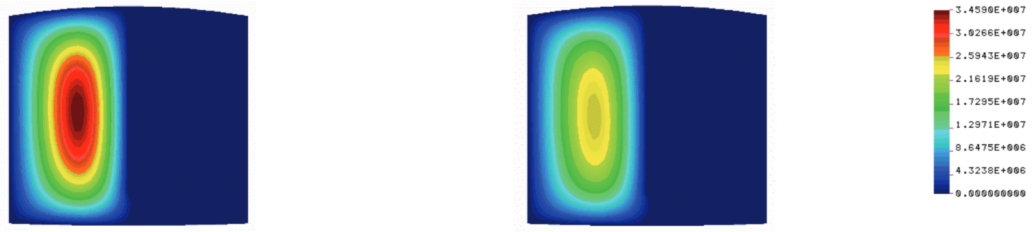

(a) (b)

FIGURE 13. Pressure field of the oil film for: (a) the isothermal assumption with T = 40° C, (b) the adiabatic assumption. Color scale from 0 to 34.6 MPa.

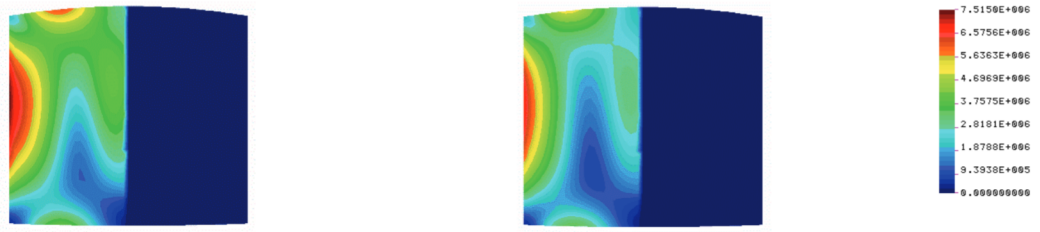

(a) (b)

FIGURE 14. Planar density of the rate of dissipative heat for: (a) the isothermal assumption with T = 40°C, (b) the adiabatic assumption. Color scale from 0 to 7.5 MW/m^2.

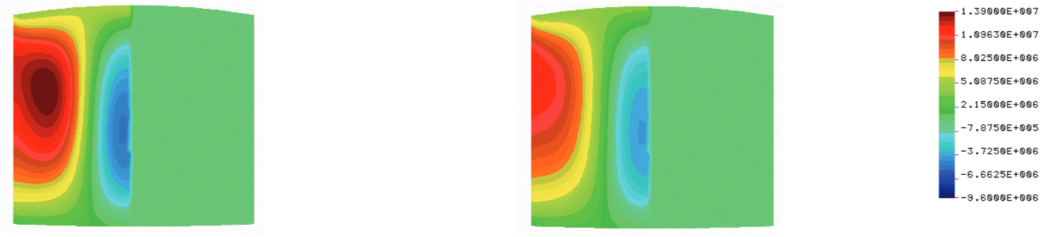

(a) (b)

(c) (d)

FIGURE 15. Planar density for the rate of working of a ring surface: (a), (c) the isothermal assumption with T = 40°C, (b), (d) the adiabatic assumption; (a), (b) the pinion, (c), (d) the wheel. Color scale from -9.6 to 13.9 MW/m^2.

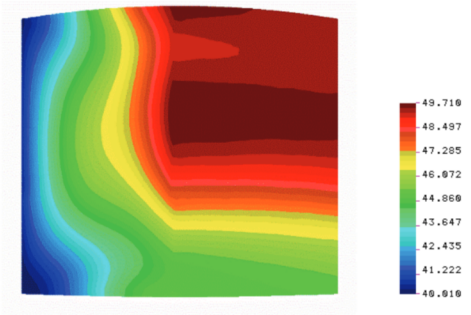

FIGURE 16. Temperature field in the adiabatic case. Color scale from 40.0 to 49.7°C.

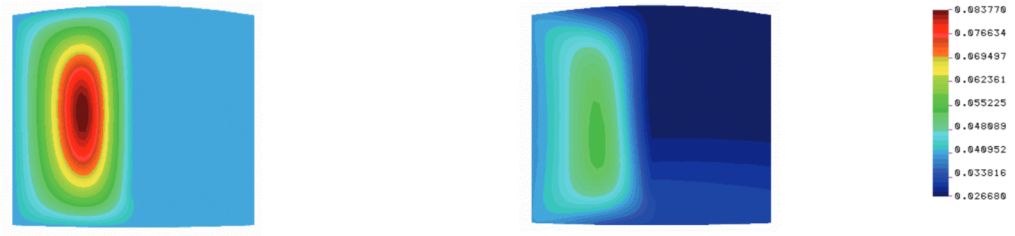

(a) (b)

FIGURE 17. Distribution of dynamic viscosity for: (a) the isothermal assumption with $T = 40°C$, (b) the adiabatic assumption. Color scale from 0.0267 to 0.0838 Pa.s.

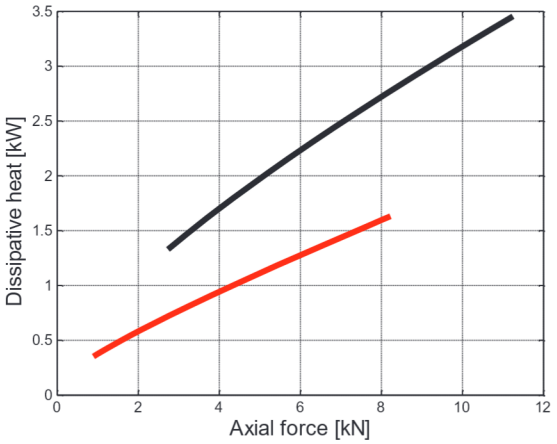

FIGURE 18. Dissipative heat versus axial contact force for the adiabatic assumption. Black – the gap between the rings filled completely (Example 1), red – the gap filled in part (Example 2).

CONCLUSION

This paper attempts to offer a better understanding of the behavior of lubricated contact between the axial rings of a high-speed gearbox under steady-state load. Mathematical modelling using the general Reynolds and energy equations and the appropriate numerical procedures are applied for this purpose. The effect of the nominal film thickness on the transmitted axial contact force and on the size of friction losses is determined for both the isothermal and adiabatic assumptions. The second assumption allows to evaluate the maximum temperature of the fluid film.

It is shown that partial filling with oil of the gap between the rings of the pinion and the wheel is more effective in reducing dissipative heat while observing the requirement for the axial force to be transmitted. This indicates that considerable attention needs to be given to the design of the oil spray inside the gearbox.

Future work will cover the design of a suitable verification experiment. However, the proposed modelling and the software created will be used to determine the parameters of the optimal design of gearbox axial rings.

ACKNOWLEDGMENTS

This study is supported by the The Technology Agency of the Czech Republic under the project “National Centre of Competence for Machinery Engineering” no. TN01000015. The authors also wish to express their gratitude to the employees of Wikov Gear Ltd. for the inspiring discussions.

REFERENCES

1. B. J. Hamrock, S. R. Schmid and B. O. Jacobson, *Fundamentals of Fluid Film Lubrication* (Second Edition, Marcel Dekker, Inc., New York, Basel, 2005).
2. O. Pinkus and B. Sternlicht, *Theory of Hydrodynamic Lubrication* (McGraw-Hill Book Company, Inc., New York, Toronto, London, 1961).
3. J. Ferron, J. Frene and R. Boncompain, ASME Journal of Lubricated Technology **105**, 422–428 (1983).
4. M. M. Khonsari, J. Y. Jang and M. Fillon, ASME Journal of Tribology **118**, 571–579 (1996).
5. B. Y. C. So and E. E. Klaus, ASLE Transactions 23(4), 409–421 (1980).
6. N. Patir and H. S. Cheng, ASME Journal of Lubricated Technology **100**, 12–17 (1978).
7. J. Voldřich and Š. Morávka, "Hydrodynamically lubricated contact of axial rings of a high-speed gearbox. Part I". Research report, University of West Bohemia, 2019 (in Czech).
8. P. A. Davidson, *Turbulence, An Introduction for Scientists and Engineers* (Second Edition, Oxford University Press, 2015).